Journal of Applied Mechanics and Technical Physics, Vol. 50, No. 4, pp. 570–575, 2009

SPATIAL DISTRIBUTION OF THE GAS PHASE IN AN AXISYMMETRIC SUBMERGED IMPACT JET

A. P. Belousov

UDC 535.8

Experimental data on the spatial distribution of the gas phase in an axisymmetric impact jet are obtained by the particle image velocimetry/laser-induced fluorescence (PIV/LIF) *method. It is shown that the distribution of bubbles in the flow is determined by the dynamics of vortex structures.*

Key words: *multiphase flows, jet flows, dynamics of the disperse phase.*

The spatial distribution of the gas phase in two-phase gas–liquid flows is an important characteristic determining the hydrodynamic structure of the flow to a large extent. The reason for this phenomenon is the fact that the presence of gas bubbles in the flow alters such characteristics of the medium as its density and viscosity. Obviously, the determining parameters in this case are the volume and distribution of the disperse phase in the examined flow region.

Based on experimental data on the distribution of the local gas content and phase velocities in the gas–liquid flow [1–8], various theoretical models were constructed, where the nonuniformity in the disperse phase distribution in the flow was determined by the nonuniformity of the pressure gradient and by the drift of gas bubbles toward the point with the minimum pressure.

To explain gas-phase migration, Zun [9] introduced a force acting on the bubble upfloating in the liquid flow with a velocity gradient. The model employs a modified solution of the problem about the motion of a rotating sphere. The angular velocity of the bubble is assumed to be proportional to the velocity gradient in the liquid.

Rouhani [10] proposed a description of the structure of the turbulent flow zone in the form of vortices moving in the flow. Interaction of these vortices and gas bubbles leads to an increase in the gas-phase concentration at places of localization of vortex structures.

The objective of the present work was an experimental study of the spatial distribution of the gas phase in an axisymmetric submerged impact jet (incident onto a flat surface at an angle of 90°) by the particle image velocimetry/laser-induced fluorescence (PIV/LIF) method [11].

A sketch of the experimental setup is shown in Fig. 1. The gas–liquid mixture circulates in a closed hydrodynamic contour including a tank with the liquid, a pump, a reservoir, and a system of pipes and transducers for monitoring the experimental parameters. A nozzle ($d = 15$ mm) is inserted through the bottom surface into a rectangular tank $200 \times 200 \times 300$ mm made of Plexiglas, so that the gas–liquid flow is incident onto the impact surface at an angle of 90°. Periodic perturbations in the flow are generated by a standard electrodynamic vibrator ESE-201 connected to the settling chamber through a sylphon bellows.

The PIV/LIF method was used as the measurement technique. A sketch of the measurement system is shown in Fig. 2. The radiation of a pulse Nd:YAG laser (second harmonic) was converted by an anamorphous optical system into a laser sheet to identify a cross section in the flow to be studied. The laser produced two consecutive pulses. Secondary emission of tracers and bubbles passed through light filters. As the tracers were fluorescent particles, the frequency of radiation scattered on these particles was lower than the frequency of laser emission. Thus, one camera registered the tracer images, and another camera recorded the bubble images. The resultant photographs were analyzed with the help of a processing system.

Kutateladze Institute of Thermophysics, Siberian Division, Russian Academy of Sciences, Novosibirsk 630090; abelousov@gorodok.net. Translated from Prikladnaya Mekhanika i Tekhnicheskaya Fizika, Vol. 50, No. 4, pp. 33–38, July–August, 2009. Original article submitted November 9, 2007; revision submitted June 23, 2008.

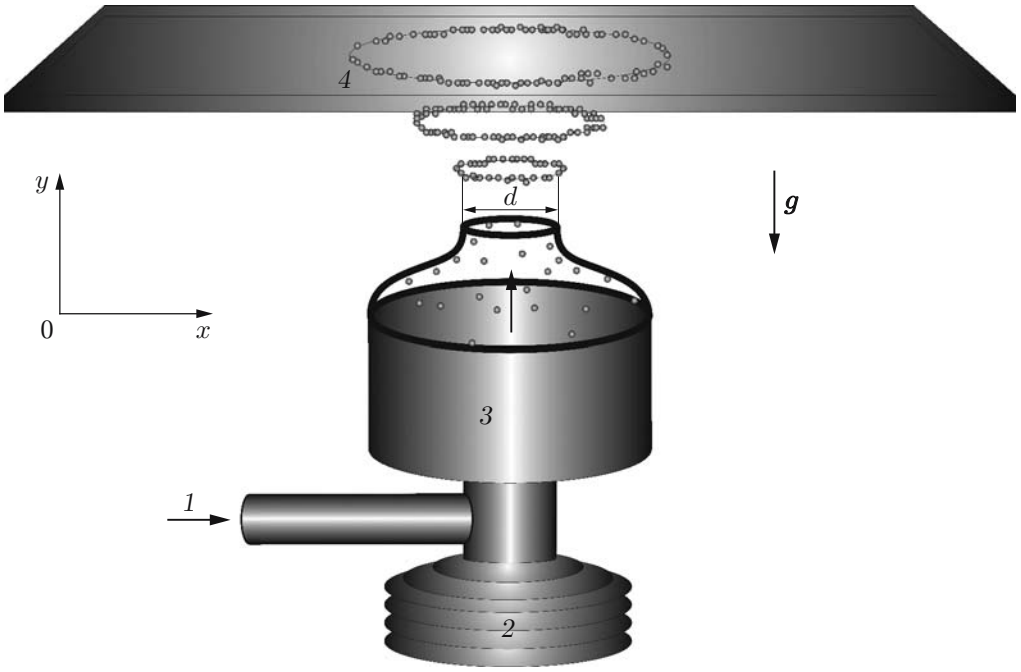

Fig. 1. Sketch of the experimental setup: 1) gas–liquid mixture; 2) ESE-201 electrodynamic vibrator; 3) nozzle; 4) impact surface.

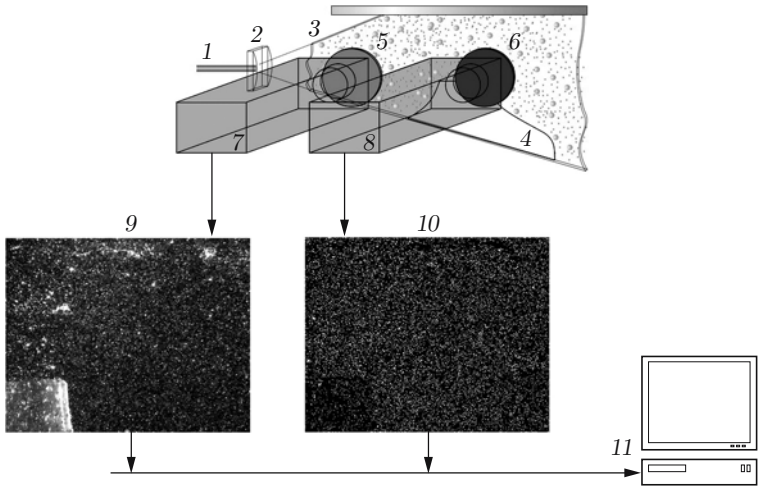

Fig. 2. Sketch of the measurement system: laser beam (1), anamorphous converter (2), laser sheet (3), nozzle (4), light filter with the maximum transmission in the green spectral range (5), light filter with the maximum transmission in the red spectral range (6), CCD cameras (7 and 8), photograph of bubbles (9), photograph of tracers (10), and system for photograph processing (11).

Correlation processing of tracer images was performed to obtain the velocity field [11]. Bubble images were used to construct the spatial distribution of the gas phase.

The bubble captured by the laser sheet has a crescent shape. According to [12], the radius of the external boundary of the image of the fluorescent volume is equal to the bubble radius; hence, the real shape of the bubble and its spatial location can be readily reconstructed.

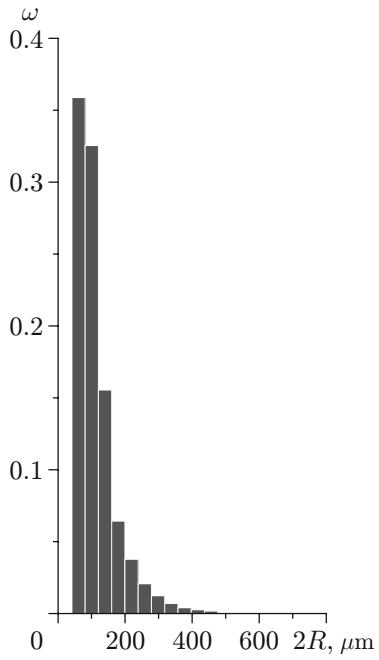

Fig. 3. Size distribution of the bubbles.

The local concentration of the gas phase in the image plane is determined by the ratio of the areas

$$\varphi_S = S_b/S_A,$$

where S_A is the area of the examined region and S_b is the area of bubbles located in this region.

The volume concentration is determined with the use of normalization coefficients calculated in the following manner. Let us denote the laser sheet width by h. Let the bubbles be spheres of radius R_j, and let their images not overlap. Then, the ratio of the concentrations φ_V and φ_S can be written as

$$\frac{\varphi_V}{\varphi_S} = \frac{4\pi}{3} S_A \sum_{j=1}^{n} R_j^3 \Big/ \left(\pi S_A h \sum_{j=1}^{n} R_j^2\right) = \frac{4}{3h} \sum_{j=1}^{n} R_j^3 \Big/ \sum_{j=1}^{n} R_j^2,$$

where n is the number of bubbles belonging to the examined region. It follows from this relation that the normalization coefficient is determined by the laser sheet width and by the fractions of the gas phase.

The methods considered above were used to study the spatial distribution of the gas phase in an impact jet saturated by the gas. The measurements were performed at the Reynolds number Re = 25,000 determined by the formula

$$\mathrm{Re} = U_0 d/\nu,$$

where ν is the kinematic viscosity of the liquid, $U_0 = 1.4$ m/sec is the mean-mass velocity of the flow, and d is the nozzle-exit diameter. Distilled water was used as the working liquid. The distance between the nozzle exit and the impact surface was $H = 30$ mm ($H/d = 2$). The PIV system had the following parameters: time between the consecutive laser pulses 20 msec, physical size of the measurement domain 53×30 mm, resolution 0.67 mm between the neighboring velocity vectors, computational domain size 32×32 pixels (1.34×1.34 mm), and laser sheet width 1 mm. The measurement error reported in [11] was smaller than 5%. The gas was injected ahead of the nozzle. The volume fraction of the gas at the nozzle exit was 1.8%. The mean bubble diameter was approximately 100 μm. A typical size distribution of the bubbles (about 150,000 measurements) is plotted in Fig. 3 (ω is the relative frequency). The measurements were performed with ordered generation of vortex structures by a periodic external action, which allowed coherent structures to be created in the flow. The frequency of this action was determined by the Strouhal number Sh = 0.5, which was the optimal value for the system used.

Figure 4 shows the spatial distribution of the gas phase averaged over 3000 realizations. Only the right half of the jet is considered owing to its symmetry. The center of the jet corresponds to the coordinate $x = 4.77$ mm.

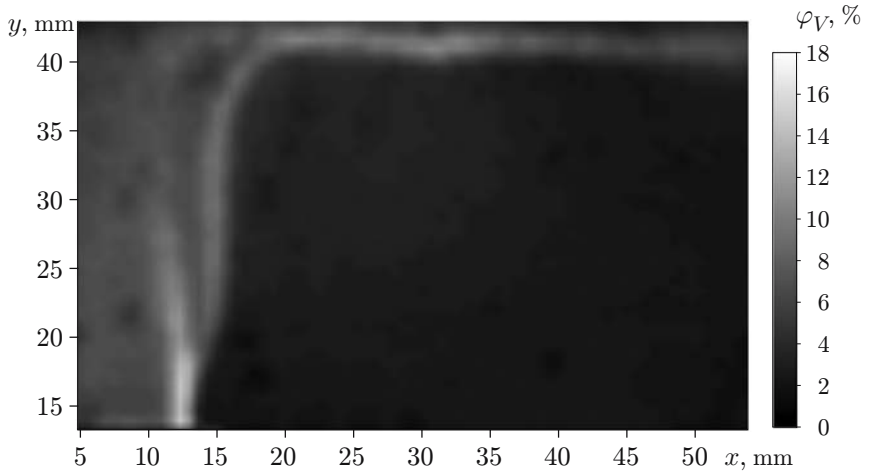

Fig. 4. Spatial distribution of the gas phase.

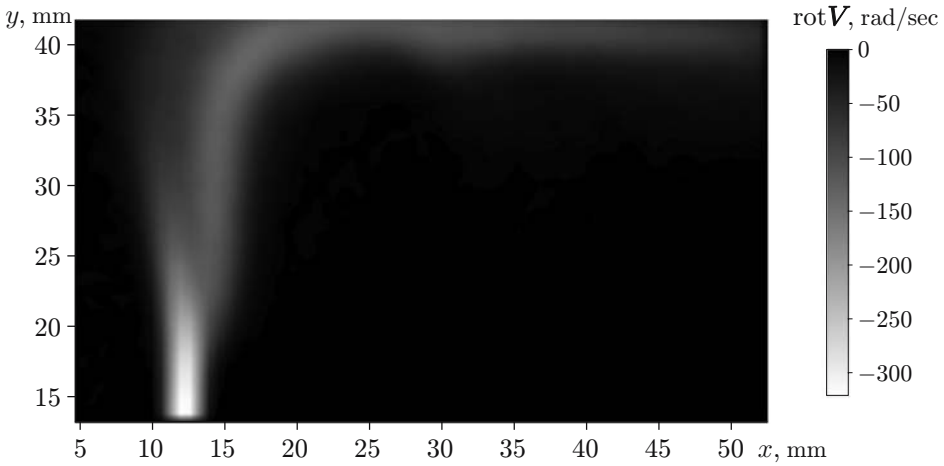

Fig. 5. Vorticity of the mean velocity field.

The upper boundary of Fig. 4 coincides with the impact surface. It is seen that the gas-phase distribution over the jet cross section is nonuniform. The maximum values are observed in the mixing layer and near the impact surface.

According to [10], the gas-phase distribution depends to a large extent on the dynamics of vortex structures. Let us determine the vorticity of the vector field of velocity $\boldsymbol{V}(x, y)$. In the Cartesian coordinate system, we obtain

$$\operatorname{rot} \boldsymbol{V} = \Big(\frac{\partial V_y}{\partial x} - \frac{\partial V_x}{\partial y}\Big)\boldsymbol{k} \tag{1}$$

(V_x and V_y are the projections of the velocity vector onto the x and y axes, respectively).

Figure 5 shows the vorticity field calculated by Eq. (1) by the finite-difference method. The velocity field used for the analysis was averaged over 3000 realizations. It is seen that the maximum of the volume concentration of the gas corresponds to the maximum value of vorticity.

Let us consider another characteristic that confirms an important role of vortex structures in hydrodynamics of multiphase mixtures. Let us construct the spatial distribution of the centers of the vortex structures on the basis of 3000 instantaneous velocity fields. For this purpose, we analyze the instantaneous velocity fields $\boldsymbol{V}(x_i, y_i)$ (x_i and y_i are the discrete coordinates of spatial points defined by the PIV system). The values of vorticity for the points (x_i, y_i) is calculated by Eq. (1). To determine the boundaries of the domain occupied by the vortex

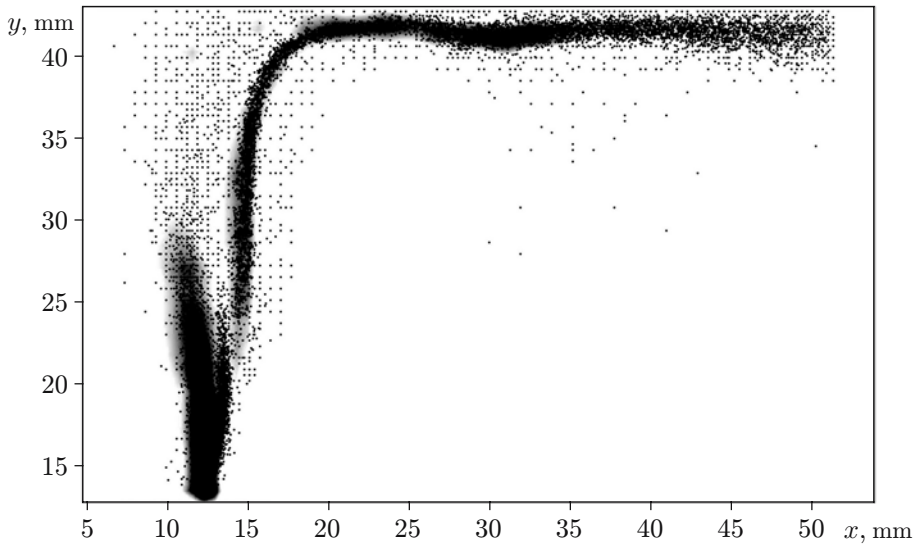

Fig. 6. Spatial distribution of the centers of the vortex structures.

structure, we choose a certain threshold value of vorticity (higher than the noise level) $I_{\text{tr}} = 0.2I_{\max}$, which allows the vortices to be clearly identified. The shape of the toroidal vortex structures in the laser sheet plane is close to a circle ($d_V \approx 4$ mm). The positions of the vortex centers are determined by the formulas

$$X = \frac{1}{N}\sum_{i=1}^{N} X_i, \qquad Y = \frac{1}{N}\sum_{i=1}^{N} Y_i,$$

where X and Y are the center coordinates, N is the number of points of the vortex structure, and X_i and Y_i are the current coordinates of the point. It is seen in Fig. 6 that the vortex centers are located in regions with an elevated concentration of the disperse phase.

Thus, the analysis of the spatial distributions of the gas phase, the mean vorticity field, and the distributions of vortex centers (see Figs. 4–6) allows us to conclude that the dynamics of vortex structures exerts the determining effect on the gas-phase distribution in an impact jet. The result obtained confirms the validity of using the advanced models [7–10] for calculating two-phase flows.

REFERENCES

1. L. G. Neal and S. G. Bankoff, "A high-resolution resistivity probe for determination of local void properties in gas–liquid flow," *AIChE J.*, **9**, No. 4, 490–494 (1963).
2. J. M. Delhaye, "Anemometrie a fil chaud dans les ecoulements diphasiques," *C. R. Acad. Sci.*, **266**, No. 6, 370–373 (1968).
3. J. M. Delhaye, "Hot-film anemometry in two-phase flow. Two-phase flow instrumentation," *Trans. ASME*, Nos. 3–6, 58–69 (1969).
4. J. M. Delhaye, "Mesure de taux de vide local en ecoulement diphasique eau-air par un anemometrie a fil claud," Rapp. TT, Centre d'Etudes Nucleaires de Grenoble, Service des Transferts Thermiques, No. 79, Grenoble (1967).
5. J. M. Delhaye, "Two-phase pipe flow," *Int. J. Chem. Eng.*, **23**, No. 3, 385–410 (1983).
6. J. M. Delhaye, R. Semeria, and J. C. Flamand, "Void fraction, vapor, and liquid temperatures local measurements in two-phase flow using a microthermocouple," *J. Heat Transfer*, **95**, No. 3, 365–370 (1973).
7. M. Kh. Ibragimov, V. P. Bobkov, and N. A. Tychinskii, "Behavior of the gas phase in a turbulent flow of a water–gas mixture in channels," *Teplofiz. Vysok. Temp.*, **11**, No. 5, 1051–1061 (1973).
8. A. Serizawa, I. Kataoka, and I. Michiyoshi, "Turbulence structure of air–water bubbly flow," *Int. J. Multiphase Flow*, **2**, No. 1, 235–246 (1975).

9. I. Zun, "The traverse migration of bubbles influenced by walls in vertical bubbly flow," *Int. J. Multiphase Flow*, **6**, No. 4, 583–588 (1980).
10. Z. Rouhani, "Effect of wall friction and vortex generation on the radial distribution of different phases," *Int. J. Multiphase Flow*, **3**, No. 1, 35–50 (1976).
11. M. Raffel, C. Willert, and Y. Kompenhans, *Particle Image Velocimetry. A Practical Guide*, Springer-Verlag, Berlin (1998).
12. A. P. Belousov and P. Ya. Belousov, "A method for measuring the size distribution and the local gas concentration in gas–liquid flows," *Optoelectr., Instrum., Data Process.*, **44**, No. 2, 131–134 (2008).